Intermediate Energy Nucleon-Antinucleon Reactions in the Quark Model

Yiharn Tzeng (曾詣涵)
Institute of Physics, Academia Sinica, Taipei, Taiwan 11529, Republic of China

(Received June 17, 1991)

Theoretical models for describing intermediate energy $N\bar{N}$ reactions in the quark degree of freedom are briefly discussed. The $N\bar{N}$ reactions are classified into three types: annihilation and productions, charge exchange, and elastic scattering, for each of which the possible lowest order diagrams are presented. We also performed calculations to determined if it is proper to include the $q\bar{q}$ annihilation and creation diagram while to ignore the multiple scattering amplitude in the elastic scattering.

I. INTRODUCTION

The nucleon-antinucleon ($N\bar{N}$) reactions can be classified into three types, namely, 1) annihilation and particle productions, examples as $N\bar{N} \rightarrow B_1\bar{B}_2$, $N\bar{N} \rightarrow M_1M_2$, and $N\bar{N} \rightarrow M_1M_2M_3$, etc., with B being a baryon and M a meson; 2) charge exchange, $p\bar{p} \rightarrow n\bar{n}$; and 3) elastic scattering, $N\bar{N} \rightarrow N\bar{N}$. Theoretical efforts to understand these processes have mainly been made through two different directions: meson exchanges[1] and quark models,[2,3] both with some extent of success.

In this short note, we limit our attention on reactions with the incident particle energy not exceeding 2 GeV so that we still stay in the intermediate energy region and not to go into the domain of high energy physics. In this energy region, experimental data indicate that the cross section of the charge exchange reaction is much smaller than those of the elastic scattering and annihilation[4 s] and also $\sigma_{ann}/\sigma_{el} \approx 2$.[6] Hence reactions of the annihilation and particle productions already dominate the $N\bar{N}$ system. This strong annihilation dominance and its great complexity in the final state productions make this system much more difficult to deal with than the nucleon-nucleon (NN) system. Also because of the particle identities' often undergoing drastic changes after interactions, people might argue that quark effects become more prominent in the $N\bar{N}$ system and hence it might be more convenient to describe the system in the quark degree of freedom. Although the QCD is produced to describe interactions in the quark degree of freedom, there is still a long way for it to become a definitely solid and practically easily applicable theory. Currently microscopic studies concerning this kind of reactions thus heavily depend on constructing some reasonable models. We wish to discuss some of these models in this short note.

II. QUARK DIAGRAMS FOR $N\bar{N}$ REACTIONS

We present in this section the most often used lowest order diagrams in the quark degree of freedom for the above various $N\bar{N}$ reactions. Shown in Fig. 1 is the production of three

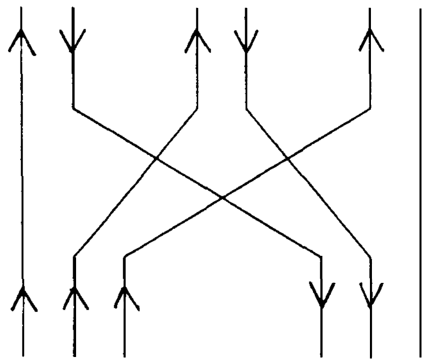

FIG 1. Three meson production from $N\bar{N}$ via the quark rearrangement model.

mesons which are formed by rearranging quarks and antiquarks into qq combinations without any annihilations among quarks and antiquarks. This is an example of the quark rearrangement model. Similar examples are the two-meson productions shown in Fig. 2 where the mesons are produced from regrouping the original quarks and antiquarks in the $N\bar{N}$ system into $q\bar{q}$ combinations while a pair of $q\bar{q}$ annihilate into either QCD vacuum or a gluon. Two meson productions can also be proceeded through annihilations and creations of qq pairs, as those shown in Fig. 3, where two $q\bar{q}$ pairs annihilate into a gluon or QCD vacuum, from which another $q\bar{q}$ pair are created to join the original $q\bar{q}$ as two mesons. Similar mechanics can be applied to baryon productions as shown in Fig. 4, which differs from Fig. 3 in having only one $q\bar{q}$ annihilation. Note that the dash line in the figure represents either a gluon or QCD vacuum which will result in different contribution to the reaction. Alberg, Henley, and Wilets[3] considered both contributions in the reaction $p\bar{p} \rightarrow \Lambda\bar{\Lambda}$ and found them in the same order of magnitude, but with different signs. These authors therefore concluded that both types of contributions should be included in the calculation.

In the above reaction, the original $u\bar{u}$ pair of $p\bar{p}$ annihilate to create an $s\bar{s}$ pair. If instead, replacing the $s\bar{s}$ pair by a $d\bar{d}$ pair or a $u\bar{u}$ pair will yield the charge exchange reaction $p\bar{p} \rightarrow n\bar{n}$

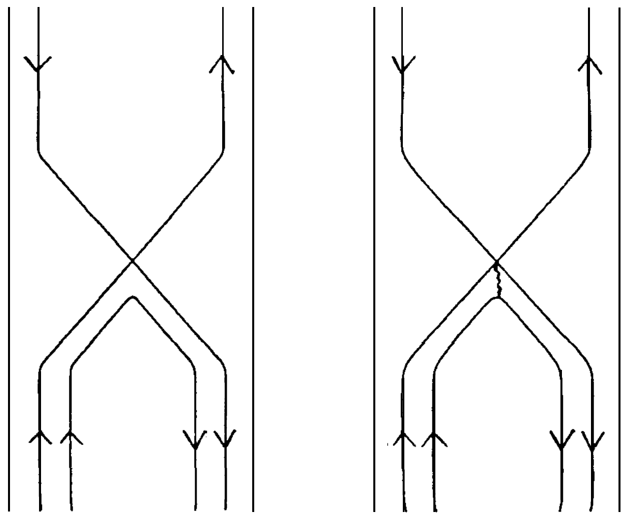

FIG 2. Two meson production from quark rearrangement in the $N\bar{N}$ system.

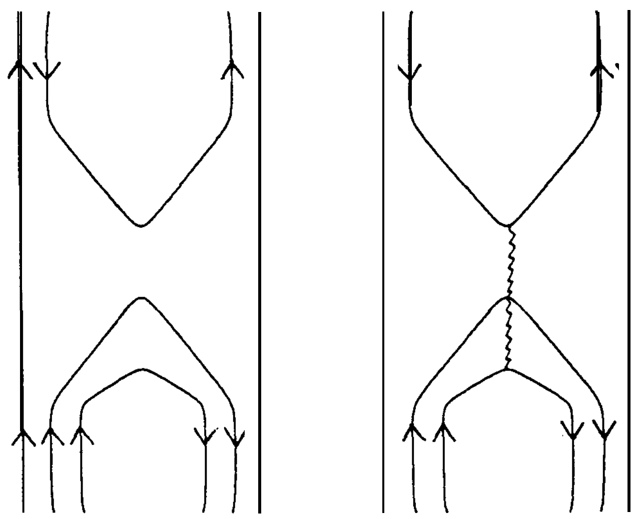

FIG 3. Two meson production from $N\bar{N}$ via $q\bar{q}$ annihilations and creation.

or the elastic scattering $p\bar{p} \rightarrow p\bar{p}$. Tegen, Mizutani, and Myhrer[7] added these quark diagrams to the OBEP, and fitted the experimental data of the charge exchange and the elastic scattering considerably well. However, before one does this kind of data fitting, one has to decide first if these types of diagrams are really the lowest order ones. Particularly in the elastic scattering, one can by no means tell without actual calculations that the contribution from Fig. 4 is really

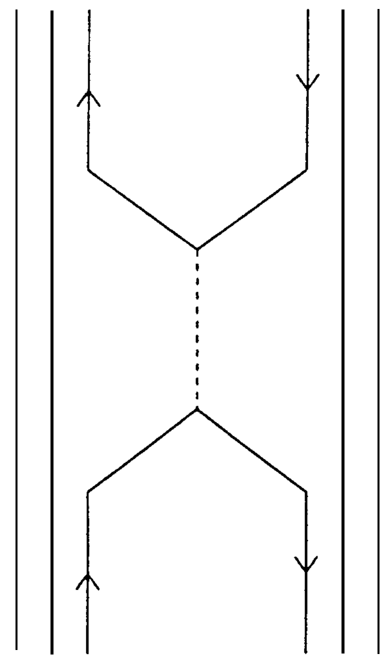

FIG 4. The $N\overline{N} \to B_1\overline{B}_2$ interaction form $q\overline{q}$ pair annihilation and creation, with the dotted line being either a gluon or the QCD vacuum.

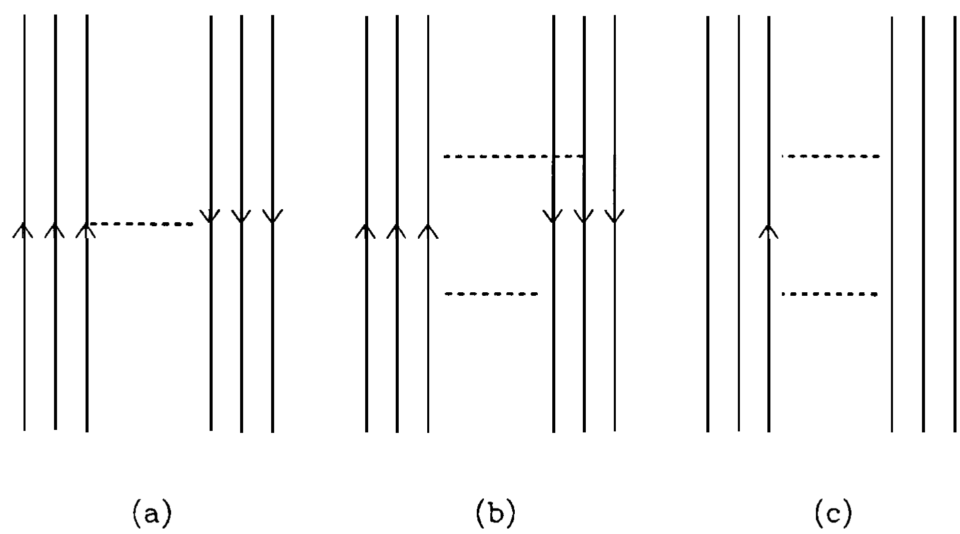

FIG 5. (a) The direct single, and (b), (c) the double scattering amplitudes with one- and two-gluon exchanges, respectively.

the most dominant one so that we can ignore contributions from other diagrams such as those shown in Fig. 5. Such calculations have recently been performed by the author[8] and will be discussed in the next section.

III. ELASTIC $N\bar{N}$ SCATTERING AND THE QUARK MODEL

Let us first examine how the diagram in Fig. 4 contributes to the $N\bar{N}$ elastic scattering. Starting from the quark-antiquark-gluon vertex

$$L_{int} = (4\pi\alpha_s)^{1/2}\bar{\psi}\gamma^{\mu}\frac{\lambda_a}{2}\psi G^a_{\mu}, \tag{1}$$

and the gluon propagator

$$D^{cc'}_{\mu\nu} = \frac{-i}{q_0^2 - \mathbf{q}^2 + i\epsilon}\delta_{cc'}\delta_{\mu\nu}, \tag{2}$$

with ψ being the quark spinor, λ_a the color SU(3) generator, G_u the gluon field, and γ_u the Dirac matrix, Faessler et al.[9] derived an $N\bar{N}$ potential up to the order of p^2/m^2 from this diagram and obtained

$$ReV_{N\bar{N}} = V_{ST}\left[\left(1 + \frac{1}{4z^2} - \frac{r^2}{24z^2b^2}\right)f(2z^2) - \frac{3}{8z^2}g(2z^2)\right]\exp(-r^2/2b^2), \tag{3}$$

$$ImV_{N\bar{N}} = -4(2)^{1/2}\pi z^3 e^{-2z^2}\left(\frac{1}{2} + \frac{1}{4z^2} - \frac{r^2}{2z^2b^2}\right)V_{ST}\exp(-r^2/2b^2), \tag{4}$$

with z = mb, m being the effective quark mass, b the nucleon size, and

$$f(\alpha^2) = \frac{4\alpha^2}{\pi^{1/2}}P\int_0^\infty \frac{x^2e^{-x^2}}{\alpha^2 - x^2}dx, \tag{5}$$

$$g(\alpha^2) = \frac{8\alpha^2}{3\pi^{1/2}}P\int_0^\infty \frac{x^4e^{-x^2}}{\alpha^2 - x^2}dx, \tag{6}$$

$$V_{ST} = \frac{\alpha_x}{324z^2b}(243 + 9\sigma_N\cdot\sigma_{\bar{N}} - 27\tau_N\cdot\tau_{\bar{N}} - 25\sigma_n\cdot\sigma_{\bar{N}}\tau_N\cdot\tau_{\bar{N}}) \cdot \left(\frac{2}{\pi}\right)^{1/2} \tag{7}$$

V_{ST} has its maximum absolute value when S = 1, T = 0. This potential turns to its nonrelativistic form as the momentum dependence is dropped,

$$V_{N\bar{N}} = V_{ST}\exp(-r^2/2b^2). \tag{8}$$

In their data fitting, Tegen et al.[7] had a similar derivation of the potential, but with a different way of parametrization. Among these various forms, we choose the convenient one in Eq. (8) for the use in later calculations. This choice is adequate for our present purpose of order of magnitude estimation, since numerical computations show that $V_{N\bar{N}}/V_{ST}$ in Eq. (8) is in the same order of magnitude as $\mathrm{Re}V_{N\bar{N}}/V_{ST}$ and $\mathrm{Im}V_{N\bar{N}}/V_{ST}$ in Eqs. (5) and (6), with only small deviations.

On the other hand, since in the constituent quark model, the $N\bar{N}$ system is treated as 3q - $3\bar{q}$ system, the multiple scattering amplitudes as those shown in Fig. 5 might have non-negligible effects in the intermediate and high energy elastic interactions. These amplitudes can be calculated from the Glauber approximation[10] which has been successfully applied to interpret medium and high energy nucleus-nucleus scattering problems. Among these amplitudes, the direct single scattering term with one-gluon exchange (as in Fig. 5(a)) vanishes for hadrons' being color singlet in nature. The double scattering amplitudes from diagrams as shown in Fig. 5(b) and 5(c), where two gluons are exchanged between the interacting $N\bar{N}$, are therefore the starting amplitudes in the Glauber multiple scattering series. Let us here use $f_1^{(2)}(q)$ to represent the sum of scattering amplitudes similar to the diagram in Fig. 5(b), and $f_2^{(2)}(q)$ the sum of those similar to the diagram in Fig. 5(c). Our main concern here is thus to find out if it is proper to include the contribution from the $q\bar{q}$ pair annihilation and creation diagram of Fig. 4, while to ignore that from $f^{(2)}(q)$, where

$$f^{(2)}(q) = f_1^{(2)}(q) + f_2^{(2)}(q), \tag{9}$$

in the data fitting of the elastic $N\bar{N}$ interaction.

In the Glauber approximation,[10] the $N\bar{N}$ elastic scattering amplitude can be expressed in terms of $q\bar{q}$ interactions as

$$F_{N\bar{N}}(q) = \sum_{n=1}^{9} f^{(n)}(q), \tag{10}$$

with the multiple scattering amplitude being

$$f^{(n)}(q) = \frac{K}{2\pi i}\int d^2b e^{i\mathbf{q}\cdot\mathbf{b}} f^{(n)}(b), \tag{11}$$

and

$$\begin{aligned} f^{(n)}(b) = & \frac{(-1)^n}{n!} \sum_{i_1,\cdots,i_n=1}^{3'} \sum_{j_1,\cdots,j_n=1}^{3'} \\ & \cdot < \Psi_i\Psi_j \left| \prod_{m=1}^{n} \Gamma_{i_m j_m}(\mathrm{b} - s_{i_m} + s_{j_m}) \right| \Psi_i(123)\Psi_j(456) >, \end{aligned} \tag{12}$$

where primes indicate summations never run over the same (i_n, j_n) pairs repeatedly, and K and **q** are, respectively, the incident momentum and the momentum transfer in the $N\bar{N}$ center of mass system, b the impact parameter, $s_{i_m}(s_{j_m})$ the transverse component of the quark ' s (antiquark ' s) position, and Γ the $q\bar{q}$ scattering profile function which is related to the $q\bar{q}$ scattering amplitude as

$$\Gamma_{lm}(b) = \frac{1}{2\pi ik} \int d^2q e^{-i\mathbf{q}\cdot\mathbf{b}} F_{lm}(q), \tag{13}$$

with k being $q\bar{q}$'s relative momentum. The nucleon (antinucleon) wave function, $\Psi_i(\Psi_j)$ is composed of three parts, namely,

$$\Psi = \Phi_R(\text{spatial})\Phi_\sigma(\text{spin} - \text{isospin})\Phi_c(\text{color}), \tag{14}$$

with the spatial part being set to be

$$\Phi_R = (3\lambda^2/\pi^2)^{3/4} \exp\{-\lambda/2[(\mathbf{r}_1 - \mathbf{r}_2)^2 + (\mathbf{r}_2 - \mathbf{r}_3)^2 + (\mathbf{r}_3 - \mathbf{r}_1)^2]\} \tag{15}$$

where $\lambda = 1/(3r_p^2)$, r_p is the nucleon size.

To evaluate $f^{(2)}(q)$ from these equations, we still need the $q\bar{q}$ amplitude $F_{lm}(q)$ which is chosen from that proposed by Richardson" who has the single gluon exchange $q\bar{q}$ amplitude for heavy quark systems to be proportional to

$$V_{q\bar{q}}(q) = \frac{\alpha_s(q)}{q^2}\left(\frac{1}{4}\lambda_q \cdot \lambda_{\bar{q}}\right), \tag{16}$$

where λ_q is the SU(3) color operator. Various QCD motivated $q\bar{q}$ amplitudes have been proposed. We choose this one simply because it can be handled with less difflculties in our case. It should also work for light quark systems.[12] For the convenience in our calculation, we set the running coupling constant for N_f flavor quarks as

$$\alpha_s(q) = \frac{12\pi}{(33 - 2N_f)\ln(q^2/\Lambda^2)}, \tag{17}$$

which was fitted to a sum of three gaussians by Godfrey and Isgur[13] with the assumption that it saturates at some value $\alpha_s^{\text{critical}}$ for low q. There they had

$$\alpha_s(q) = \sum_{i=1}^{3} a_i e^{-b_i q^2} \tag{18}$$

with $(a_1, a_2, a_3) = (0.25,\ 0.15,\ 0.20)$, and $(b_1, b_2, b_3) = (1,\ 0.1,\ 0.001)(\text{GeV}/c)^{-2}$. This was used in Ref. 13 to describe a wide range of mesons. To obtain convergent results for small q in the calculation of $F^{(2)}(q)$, we further modify $1/q^2$ of Eq. (16) into

$$1/q^2 \rightarrow \int_0^\infty e^{-xq^2} e^{-ax^2} dx, \tag{19}$$

with $a^{1/4}$ acting as a cut-off mass serving to avoid any possible arising of unphysical Van der Waals forces[14] from iterated confining interactions. Mathematically, the integral becomes exactly $1/q^2$ as a = 0. After the expectation values of color parts being evaluated, " $f_1^{(2)}(q)$ and $f_2^{(2)}(q)$ can then be readily computed through double-x integrations. This double scattering amplitude $f^{(2)}(q)$ is then compared with that arising from the qq annihilation and creation potential of Eq. (8), in which the same parameters as those in Ref. 9 are used in the following comparisons, i.e., m = 300 MeV/c^2, α_s = 1.39, except we set b = r_p = 0.6 and 0.83 fm. The $N\bar{N}$ incident energy is set to be 1 GeV as an example. Similar results are expected as the energy varies around the intermediate energy domain where the Glauber approximation should be valid.

The results of these calculations are shown in Figs. 6 and 7 with r_p = 0.6 and 0.83 fm and a = 0.1, 0.01 fm^{-4}. At the same a, $if^{(2)}(q)$ and $f_{ann}(q)$, the amplitude calculated from Eq. (8) via the Born approximation at its maximum magnitude of S = 1, T = 0, both have a common feature, that the one with a smaller r_p has a smaller slope. At small q, $if^{(2)}(q)$ increases with

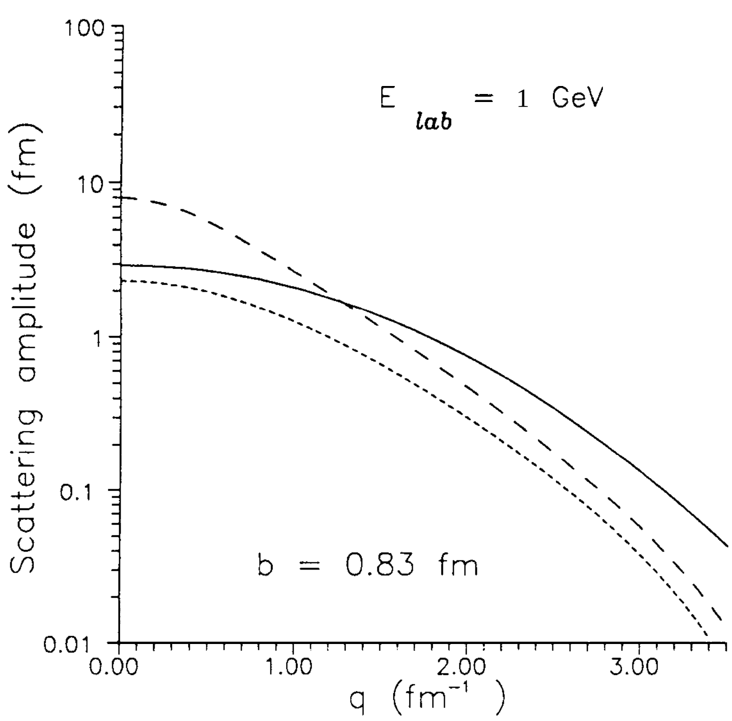

FIG 6. Comparison of $if^{(2)}(q)$ (the dotted line for a = 0.1 fm^{-4} and the dashed one for a = 0.01 fm^{-4}) and $-f_{ann}(q)$ (the solid line) with b = r_p = 0.83 fm, at E_{lab} = 1 GeV.

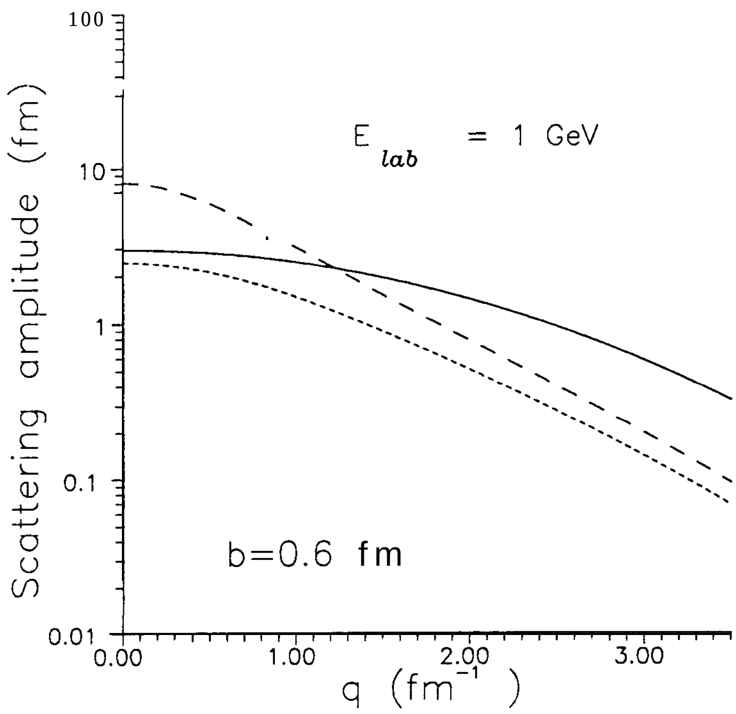

FIG 7. Same as Figure 6, except b = r_p = 0.6 fm.

decreasing a, due to the $q\bar{q}$ amplitude's getting stronger with smaller a. Consequently, other higher order terms in Eq. (10) also become stronger. According to the general characteristics of the Glauber series, destructive interferences among $f^{(2)}(q)$ and these terms usually occur and will bring down the resultant amplitude accordingly. Though other higher order terms are not added together at this moment, a crude comparison of $f^{(2)}(0)$ with the experimental total cross section $\sigma_{tot} d\sigma/d\Omega$ $(\theta = 0)^6$ seems to forbid the parameter *a* to

r_p, if $f^{(2)}(q)$ is about the same order of magnitude as $-f_{ann}(q)$. None of these calculated cases show negligible $f^{(2)}(q)$ as compared to $f_{ann}(q)$. The relativistic corrections made in Ref. 9 enhances $f_{ann}(q)$ a little bit, but not large enough to revise this result. If one puts in the realistic $N\bar{N}$ relative motion, $f_{ann}(q)$ will be suppressed even more.

IV. CONCLUDING REMARKS

We have presented in this short note some theoretical models for intermediate energy $N\bar{N}$ reactions in the quark degree of freedom. Since our purpose here is not to tit the experimental data quantitatively, the discussion is rather qualitative. Nevertheless, it provides some information about how this complicated $N\bar{N}$ is treated theoretically.

We have particularly performed numerical comparisons on the amplitude from the two-gluon exchange diagrams with that derived by Faessler et al.[9] from the $q\bar{q}$ pair annihilation and creation diagram and found that none of our calculated cases show a negligible contribution from any of these two different kinds of amplitudes as they being compared with each other. Hence on this point we conclude that much more careful considerations should be taken in choosing the quark diagrams before one tries to fit experimental $N\bar{N}$ elastic scattering.

ACKNOWLEDGMENTS

This work was supported in part by a grant from the National Science Council of the Republic of China.

REFERENCES

1. For examples, F. Tabakin and R. A. Einstein, Phys. Rev. C31, 1857 (1985); M. Kohno and W. Weise, Phys. Lett. **B179, 15** (1986).
2. For examples, S. Furui and A. Faessler, Nucl. Phys. **A468, 669** (1987); M. Maruyama, S. Futui and A. Faessler, ibid, **A472, 643** (1987); G. Ihle, H. J. Pirner and J. M. Richard, ibid, **A485, 481** (1988); M. Burkardt and M. Dillig, Phys. Rev. **C37, 1362** (1988).
3. M. A. Alberg, E. M. Henley and L. Wilets, Zeit. Phys. **A331, 207** (1988); Phys. Rev. **D38, 1506** (1988).
4. A. S. Clough et al., Phys. Lett. **146B,** 299 (1984).
5. K. Nakamura et al., Phys. Rev. Lett. 53,885 (1984).
6. R. A. Kunne et al., Nucl. Phys. **B323, 1** (1989).
7. R. Tegen, T. Mizutani and F. Myhrer, Phys. Rev. **D32, 1672** (1985).
8. Yiharn Tzeng, Journ. of Phys. G: Nucl. Part. Phys. **17, 221** (1991).
9. A. Faessler, G. Lübeck and K. Shimizu, Phys. Rev. **D26, 3280** (1982).
10. R. J. Glauber, in Lectures in Theoretical Physics, edited by E. Britten and L. G. Dunnham (Interscience, New York, 1959) Vol. I. p 315.
11. J. L. Richardson, Phys. Lett. **82B,** 272 (1979).
12. Chun Wa Wong, Phys. Rep. **136, 1** (1986).
13. S. Godfrey and N. Isgur, Phys. Rev. **D32,** 189 (1985).
14. For examples, R. S. Willey, Phys. Rev. **D18, 270** (1978); 0. W. Greenberg and H. J. Lipkin, Nucl. Phys. **A370, 349** (1981); H. J. Lipkin, Phys. Lett. **B113, 490** (1982); Th. Pfenninger, A. Faessler and K. Bräuer, Nucl. Phys. **A466, 495** (1987); Th. Pfenninger and A. Faessler, ibid, **A484, 476** (1988).
15. Yiharn Tzeng, Phys. Rev. **C36, 277** (1987).